Nano-Structures & Nano-Objects 7 (2016) 41–48

Contents lists available at ScienceDirect

Nano-Structures & Nano-Objects

journal homepage: www.elsevier.com/locate/nanoso

Plasma afterglow-assisted oxidation of iron–copper bilayers

A. Imam [a], T. Gries [a,b], H. Sezen [c], M. Amati [c], D. Mangin [a], T. Belmonte [a,b,*]

[a] *Université de Lorraine, Institut Jean Lamour, UMR CNRS 7198, NANCY, F-54042, France*
[b] *CNRS, Institut Jean Lamour, UMR CNRS 7198, NANCY, F-54042, France*
[c] *Elettra - Sincrotrone Trieste S.C.p.A. S.S. 14 km 163,5 in AREA Science Park, 34149 Basovizza, Trieste, Italy*

HIGHLIGHTS

- Iron–copper bilayers are deposited by magnetron sputtering
- Bilayers are oxidized by plasma afterglow at atmospheric pressure
- Caterpillar-like patterns covered by CuO and Fe_2O_3 nanostructures are formed
- Copper comes up through cracks or Fe_2O_3 layer made permeable by tensile stress
- Localizing nanowires is achievable by creating crack patterns before oxidation.

GRAPHICAL ABSTRACT

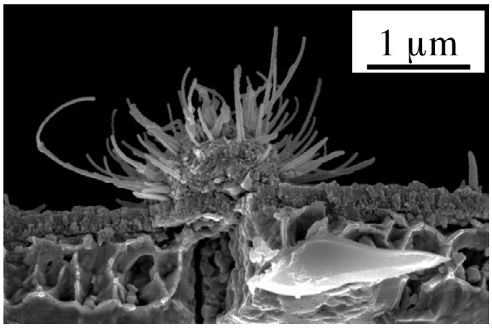

Caterpillar-like pattern covered by CuO and Fe_2O_3 nanostructures

ARTICLE INFO

Article history:
Received 14 April 2016
Received in revised form
11 June 2016
Accepted 12 June 2016

Keywords:
CuO
Fe_2O_3
Cu/Fe stacks
Nanostructuration
Afterglow
Oxidation

ABSTRACT

Iron layers with variable thicknesses, deposited onto copper thin films, are oxidized by a plasma afterglow at atmospheric pressure. Such a bilayer arrangement enables the growth of caterpillar-like patterns covered by CuO and Fe_2O_3 nanostructures. Two main mechanisms are at stake: either copper comes up to the surface through cracks or boundaries between the columns of the coating, or it diffuses through parts of the Fe_2O_3 layer made permeable by tensile stress. Structures grown by the former mechanisms are characterized by a central channel, whereas those grown by the latter exhibit a plane interface above which stands an equiaxed grain heap. This result was used to localize the growth of nanowires in cracks formed priory to the afterglow-assisted treatment. By resorting to XPS microscopy experiments carried out with the scanning photoelectron microscope at the ESCAMicroscopy beamline of the Elettra synchrotron facility in Trieste, we could gain access to the surface composition of a single isolated pattern.

1. Introduction

Growing tailored oxide nanostructures is of major importance in some applications like water splitting [1–3] or catalysis [4–6]. It might be useful to control the way a surface could be patterned by nanostructures with well-defined properties. Resorting to non-equilibrium media, like direct plasmas or afterglows, opens up new opportunities to control the synthesis of nanostructures [7]. In direct low-pressure plasma processes, sputtering mechanisms can be partly responsible for the growth of nanostructures [8–10]. In plasma afterglow processes, oxygen atoms or metastable states of oxygen – mainly the singlet state $O_2(a^1\Delta_g)$ – are available. They are more active than ground state oxygen at low temperature because of the extra amount of energy coming from dissociation or

---

[*] Corresponding author.
E-mail address: thierry.belmonte@univ-lorraine.fr (T. Belmonte).

http://dx.doi.org/10.1016/j.nanoso.2016.06.003

excitation. As low-temperature oxidation favours anisotropic crystal growth, and thus, the synthesis of nanostructures, non-equilibrium media promotes the growth of oxide nanostructures [11–16].

In a recent work [17], we showed that mixing iron and copper in alloy thin films strongly affects the growth processes of nanostructures, leading to original shapes. Oxidation of copper, because it is slower than iron, is strongly anisotropic, leading easily to nanostructures. Increasing the amount of iron decreases the level of stress in the film and hinders but never stops the access of copper to the topmost surface.

Thermal oxidation of brass alloys in air was investigated by Zhu et al. [18]. They could simultaneously synthesize ZnO–CuO nanostructures between 623 and 813 K. By varying the brass composition, 1D nanowires/nanoflakes, 2D nanosheets, and 3D networks could be grown. Another group studied the influence of the oxygen partial pressure [19] and found that the compressive growth stress causes the plastic deformation of oxide scale and increases dislocation defects in scale, which is of benefit to the growth of nanowires and nanowalls. In a previous paper [20], the same authors described that the increase in oxidation temperature from 773 to 873 K typically increases the compressive growth stress. As plastic deformation is easier in the substrate than that in the oxide scale, buckling-induced patterns decrease in size, whereas micro-cracks form in the oxide scale. Micro-cracks act as short-circuits, resulting in the formation of flower-like nanostructures.

Finally, let us mention that radiofrequency plasma-assisted oxidation of brass was reported [21] but no nanostructures were formed in the studied conditions.

In the present work, we investigate the role of an iron thin film with variable thickness on the access of copper to the topmost surface. Fe/Cu bilayers are oxidizing with an Ar–O_2 plasma afterglow operating at atmospheric pressure. Cu/Fe bilayers were also investigated but the corresponding results are not reported hereinafter, in so far as thus-grown nanostructures are similar to those formed with Cu-rich alloys and reported in Ref. [17].

2. Experimental set-up

The experimental set-up was described in details elsewhere [17]. Briefly, an atmospheric Ar–O_2 microwave plasma was ignited in a fused silica tube (27 mm inner diameter) placed in a 2.45 GHz resonant cavity. The power absorbed by the plasma was 100 W. Flow rates of gases were controlled by mass flow controllers and the total flow rate was 275 sccm (standard cubic centimetre per minute). The partial pressure of oxygen in the gas mixture was set at 9.1 vol.%. The treatment time was 2 h to get sufficiently long structures to identify and characterize them as clearly as possible. The micro-afterglow was visible as a light beam escaping a hole (500 μm in diameter) drilled in a brass plate screwed on one wall of the cavity [11]. Oxidizing active species in the afterglow are mainly O, O_2(a) and O_2(X) because the afterglow is too hot to allow the formation of O_3 [12].

A detailed thermal analysis reported in Ref. [17] showed that the maximum treatment temperature is about 733 K. When the plasma afterglow hits the metallic surface, it oxidizes concentric areas that extend radially up to several millimetres. Because of the temperature radial gradient that prevails in such conditions, Fe/Cu thin films, when submitted to the afterglow treatment, produce different nanostructures from the centre of the treatment outward, for a given thickness ratio.

Samples were Fe/Cu films deposited by DC magnetron sputtering. Thicknesses of copper and iron layers were set by adjusting the deposition time. The thickness of the bilayer was 1.3 μm. The iron layer, always deposited onto the copper layer, had thicknesses of 50, 155 and 900 nm. The base vacuum in the sputtering chamber is 5×10^{-6} mbar. The distance between the sample, made of fused silica, and the targets (50 mm in diameter, 3 mm thick and >99.99% purity for Cu target and 0.25 mm and 99.5% purity for Fe target) was 100 mm. The substrate-holder rotated at 28 revolutions per minute during deposition to ensure homogeneity. Thin films were deposited at a pressure of 5.8×10^{-3} mbar in a 10 vol% H_2—90 vol% Ar mixture.

Treated surfaces were characterized by several surface diagnostics. Scanning Electron Microscopy (SEM) was made with a Philips XL 30. X-ray diffraction using Cu-Kα radiation ($\lambda = 0.179026$ nm) was performed with a Bruker D8 Discover diffractometer.

A CAMECA IMS 7F instrument was used for Secondary Ion Mass Spectrometry (SIMS). A Cs^+ primary ion beam of 30 nA operating at 5 kV was used to sputter sample with an impact energy of 3 keV. Mass Resolving Power was set to 2000. Depth-profiles were acquired over an area of 100 × 100 μm^2.

The XPS microscopy experiments were carried out with the scanning photoelectron microscope (SPEM) at the ESCAMicroscopy beamline at the Elettra synchrotron facility in Trieste, Italy. In SPEM, the incident X-ray beam, with 648.5 eV photon energy, is focused on the sample to a spot of 130–150 nm diameter using zone plate optics. The sample is then scanned under the focused beam. The highest cross-section peaks of Cu 2p and Fe 2p are not accessible with such a photon energy, but Cu 3p and Fe 3p could be acquired. The SPEM instrument has two operation modes, microprobe photoelectron spectroscopy and spectromicroscopy imaging. The microprobe spectroscopy mode is identical to conventional XPS spectroscopy, *i.e.* energy distribution curves are measured from the selected area illuminated by a 130 nm focused beam with a 0.2 eV spectral resolution. The imaging mode maps the surface distribution of elements by collecting photoelectrons with a selected energy window while scanning the specimen with respect to the focused beam. More details about the instrument can be found in Ref. [22].

3. Results and discussion

3.1. Layer and patterns structures

In Fig. 1, a map of the different nanostructures obtained with the afterglow process for iron thicknesses ranging from 50 to 900 nm is depicted. Four main types of nano-objects are found: Fe_2O_3 nanoblades, CuO nanowalls, nanotowers and nanowires. These nano-objects are described in details in [17]. Briefly, CuO nanowalls are characterized by their thickness, which is much larger than Fe_2O_3 nanoblades (∼50 nm vs. ∼10 nm), their height, which is always lower than nanoblades for given conditions, and by the existence of amorphous domains embedded in a crystalline matrix (which is not observed with Fe_2O_3 nanoblades). Nanotowers are an assembly of two nanowires with an amorphous phase in between. When the width of the nanostructure shrinks, large steps appear, producing a serrated shape as in a tower. CuO nanowires with diameters as small as 5 nm are also obtained.

The presence of the iron layer on top of the copper layer leads to the formation of caterpillar-like patterns (Figs. 2 and 3), especially in the external part of the radial distribution (Fig. 1). In Fig. 2, we show that each caterpillar-like pattern can be covered by different types of nanostructures, as indicated in Fig. 1, *i.e.*Fe_2O_3 nanoblades, CuO nanowalls, nanotowers and nanowires, depending on the temperature. Fe_2O_3 nanoblades are very easy to distinguish from other nanostructures, which makes finally all nanostructures easily recognizable.

Patterns get sparser and shorter when thickness of the iron layer is increased. It is important to consider that patterns only appear if the temperature is low enough, which seems to depend